Turbulence Modeling Course's Term-project

Lattice-Boltzmann Method for Turbulent Flow Simulation

Instructor:

Professor M. Taeibi Rahni

Teaching Assistant:

Dr. Y. Jafari

Student:

Dina Soltani Tehrani

Spring 2022

Table of Contents

Introduction

From a physics standpoint, the primary motivation for developing new methods for simulating fluid dynamics that use a discrete, pseudo-microscopic approach, such as Lattice-Gas Automata (LGA) or the Lattice-Boltzmann method (LBM) and its derivatives, is that the dynamics are simpler and more general than the continuum approach. A computational benefit over traditional approaches can be obtained by reducing the underlying physics such that just the important aspects (conservation laws, symmetry requirements, correct equilibrium distributions) required to ensure accurate macroscopic behavior are kept. In this regard, the LGA and Lattice Boltzmann (LB) approaches have been implemented in a variety of flow physics fields, such as directly simulated or modeled single-phase turbulent flows, flows in complex geometries, multiphase and multicomponent flows, and flows undergoing heat transfer and chemical reactions.

In this work, we focus on incorporating the algebraic Prandtl's Mixing Length Model for turbulence simulation based on the Lattice-Boltzmann Method. The case of our study is the flow around a circular cylinder for different Reynolds numbers, resulting in the study of different flow regimes around the cylinder.

Overview of The Fluid Simulation Method

Introduction Into the Lattice-Boltzmann Method

This introductory section into the LBM have been written based on the author's understandings and selected parts from the literature [1].

The Lattice Boltzmann Approach is a modern approach in Computational Fluid Dynamics. The Boltzmann Equation is the equation at the molecular level, that from its averaging, the Navier-Stokes equations have resulted. This equation is able to capture a larger number of physical phenomena at the molecular level of description, rather than at the hydrodynamic level of the Navier-Stokes equations. Not being subject to a separation of time scales, the Boltzmann equation has the ability to describe fluids in non-hydrodynamic regimes with large molecular mean free paths. The equation is also able to capture transport phenomena such as friction, diffusion, temperature transport, and etc.

The Lattice Boltzmann approach has noticeable advantages:

- It is easy to apply for complex domains,
- easy to treat multi-phase and multi-component flows without a need to trace the interfaces between different phases,
- it can be naturally adapted to parallel processes computing,
- although it needs more computer memory compared with NS solver, it is not a big constraint compared to the MD approach,
- it can handle a problem in micro- and macro-scales with reliable accuracy.

In traditional computational fluid dynamics methods (CFD), Navier–Stokes equations (NS) solve mass, momentum and energy conservation equations on discrete nodes, elements, or volumes. In other words, the nonlinear partial differential equations convert into a set of nonlinear algebraic equations, which are solved iteratively. In LBM, the fluid is replaced by fractious particles. These particles stream along given directions (lattice links) and collide at the lattice sites. The LBM can be considered as an explicit method regarding the locality of the collision and streaming processes.

The primary computational element in the Lattice Boltzmann approach is the particle occupation, also known as the distribution function, in discrete phase space (space, velocity, time and energy are all discretized). Statistical Mechanics explain and predict how the properties of atoms and molecules (microscopic properties) determine the phenomenological (macroscopic) properties of matter such as the viscosity, thermal conductivity, and diffusion coefficient. The distribution function (probability of finding particles within a certain range of velocities at a certain range of locations at a given time) replaces tagging each particle, as in molecular dynamic simulations. The method saves the computer resources drastically.

Lattice Boltzmann Method, More in Details.

A statistical description of a system can be explained by distribution function *f(r, c, t)*; where *f(r, c, t)* is the number of molecules at time *t* positioned between *r* and *r* + *dr* which have velocities between *c* and *c* + *dc*. In Eulerian methods, we consider a control volume or control mass to tag the molecules under study; however, in LBM, which can be considered as a Lagrangian method, we consider a molecule as if it is under our study when its velocity is within a certain range, and its location is within a certain range, at an instant of time. An external force *F* acting on a gas molecule of unit mass will change the velocity of the molecule from *c* to *c* + *Fdt* and its position from *r* to *r* + *cdt*.

The number of molecules before applying the external force is equal to the number of molecules after the disturbance if no collisions take place between the molecules. It is understandable that when two solid balls collide with each other, the velocity magnitude and direction of both of the balls change. That is why we say that if collisions take place between the molecules there will be a net difference between the numbers of molecules in the interval *drdc*, with the velocity within our certain range. The rate of change between final and initial status of the distribution function is called collision operator, Ω.

Hence, the equation for evolution of the number of the molecules can be written as,

$$\frac{df(x,c,t)}{dt} = \Omega(f(x,c,t)) \qquad \text{(Eq. 1)}$$

$$\frac{df(x,v,t)}{dt} = \frac{\partial f}{\partial r}\frac{d\boldsymbol{r}}{dt} + \frac{\partial f}{\partial c}\frac{dc}{dt} + \frac{\partial f}{\partial t} \qquad \text{(Eq. 2)}$$

where the vector **r** can be expressed in 3-D Cartesian coordinate system as **r** = x*i* + y*j* + z*k*.

The above equations state that the total rate of change of the distribution function is equal to the rate of the collision.

Equation (Eq. 11) can be written as,

$$\frac{df(x,v,t)}{dt} = \frac{\partial f}{\partial r}\boldsymbol{c} + \frac{\partial f}{\partial c}\boldsymbol{a} + \frac{\partial f}{\partial t} \qquad \text{(Eq. 3)}$$

where $\boldsymbol{a}$ is the acceleration and can be related to force $\boldsymbol{F}$ by Newton's second law, $a = F/m$. Therefore, the Boltzmann transport equation (Eq. 10) can be written as,

$$\frac{\partial f}{\partial r}\cdot\boldsymbol{c} + \frac{F}{m}\cdot\frac{\partial f}{\partial c} + \frac{\partial f}{\partial t} = \Omega(f(x,c,t)) \qquad \text{(Eq. 4)}$$

The $\Omega(f(x,c,t))$ is a function of *f* and need to be determined to solve the Boltzmann equation.

Note that, for systems without an external force, *F*, the Boltzmann Equation can be written as,

$$c \cdot \nabla f + \frac{\partial f}{\partial t} = \Omega(f(x,c,t)) \quad \text{(Eq. 5)}$$

Equation (Eq. 13) is an advection equation with a source term ($\Omega(f)$), or advection with a reaction term, which can be solved exactly along the characteristic lines that is tangent to the vector *c*, if $\Omega(f)$ is explicitly known. The problem is that Ω is a function of *f* and (Eq. 13) is an integro-differential equation, which is difficult to solve. Other than that, if we can come up with the solution to such an equation, we can write the conservation of mass, momentum, and energy as follows:

Conservation of Mass $$\rho(r,t) = \int m\, f(r,t,c)\, dc \quad \text{(Eq. 6)}$$

Conservation of Momentum $$\rho(r,t)u(r,t) = \int m\, c\, f(r,t,c)\, dc \quad \text{(Eq. 7)}$$

Conservation of Energy $$\rho(r,t)e(r,t) = \int m\, (c-u)^2\, f(r,t,c)\, dc \quad \text{(Eq. 8)}$$

where m is the molecular mass and u_a the particle velocity relative to the fluid velocity, the peculiar velocity, $u_a = c - u$.

It is difficult to solve Boltzmann equation because the collision term is very complicated. The outcome of two body collisions is not likely to influence significantly, the values of many measured quantities. Hence, it is possible to approximate the collision operator with simple operator without introducing significant error to the outcome of the solution.

The collision operator is suggested to be replaced as,

$$\Omega(f) = \omega\,(f^{eq} - f) = \frac{1}{\tau}\,(f^{eq} - f) \quad \text{(Eq. 9)}$$

The coefficient ω is called the collision frequency and τ is called relaxation factor. The local equilibrium distribution function is denoted by f^{eq} which is Maxwell–Boltzmann distribution function. The approximation above is called the BGKW approximation for the collision operator.

After introducing BGKW approximation for the collision operator, the Boltzmann equation ((Eq. 5), without external forces) can be approximated as,

$$c \cdot \nabla f + \frac{\partial f}{\partial t} = \frac{1}{\tau}\,(f^{eq} - f) \quad \text{(Eq. 10)}$$

Solving the equation above, (Eq. 18), is called the Lattice-Boltzmann Method. In this method, the above equation is discretized and assumed it is valid along specific directions, linkages.

The discrete Boltzmann equation can be written along a specified direction as,

$$c_i \cdot \nabla f_i + \frac{\partial f_i}{\partial t} = \frac{1}{\tau}\left(f_i^{eq} - f_i\right) \quad \text{(Eq. 11)}$$

The above equation, (Eq. 19) is the working horse of the lattice Boltzmann method and replaces Navier–Stokes equation in CFD simulations.

Note some comments about the (Eq. 19):

1. The equation is a linear partial differential equation.
2. The equation looks like an advection equation with a source term.
3. The right-hand side of the equation represents the advection (streaming).
4. The left-hand side term represents the collision process, source term.

The BGKW approximation for the collision operator is the simplest choice. In fact, the key element in applying LBM for different problems is the equilibrium distribution function, f^{eq}, which is governed by the choice for the collision operator, and the source term, if existed. The procedure of solving diffusion, advection–diffusion, momentum, and energy equations is the same. The difference mainly depends on the equilibrium distribution function. In fact, different physical problems (such as a wave propagation problem, etc.) can be solved by LBM provided that a proper equilibrium distribution function is used.

In LBM, the solution domain needs to be divided into lattices. At each lattice node, the factitious particles (distribution function) reside. Some of these particles, stream (move) along specified directions to the neighboring nodes. The number of directions, call them linkages, depends on the lattice arrangement. The common terminology used in LBM is to refer to the dimension of the problem and the number of speeds is using **DnQm**, where n represent the dimension of the problem (1 for 1-D, 2 for 2-D and 3 for 3-D) and m refers to the speed model, number of linkages.

Turbulence Modelling

One of the beneficial properties of microscopic methods is that characteristics of the flow that are functions of gradients of conserved quantities, which would require nonlocal operations to compute using the continuum partial differential equation approach, can be computed from higher order moments of the distribution function. Two examples of this are the stress tensor, $\Pi = \sum_{ji} \boldsymbol{c}_{ji}\boldsymbol{c}_{ji}N_{ji}$, and the energy flux. Concentrating on the stress tensor, we see that this term can be split into a Euler component, and a dissipative component, based on the Chapman-Enskog Analysis [16].

The Chapman-Enskog theory provides a framework for deriving hydrodynamic equations for a gas from the Boltzmann equation. The technique validates otherwise phenomenological constitutive relations found in hydrodynamical descriptions like the Navier-Stokes equations. Thus, expressions for various transport coefficients such as thermal conductivity and viscosity in terms of molecular parameters are obtained. As a result, Chapman-Enskog theory is an important step in transitioning from a microscopic, particle-based description to a continuum hydrodynamical one. The base theory is named after Sydney Chapman and David Enskog, who independently proposed it in 1916 and 1917. In this paper, we would not get into the details of the theory, while the interested reader may find the details in the literature [16].

Continuing our study, the stress tensor will have the following form, derivable from standard Chapman–Enskog analysis:

$$\Pi = \Pi^{(0)} + \left(1 - \frac{\omega}{2}\right)\Pi^{(1)} \qquad \text{(Eq. 12)}$$

$$\Pi^{(0)} = P\mathbf{I} + \rho\mathbf{u}\mathbf{u} \qquad \text{(Eq. 13)}$$

$$\Pi^{(1)} = -{}^{2P}/_{\omega}\frac{1}{2}\left[\frac{\partial u_\beta}{\partial x_\alpha} + \frac{\partial u_\alpha}{\partial x_\beta} - \frac{2}{\mathbf{D}}(\nabla.\mathbf{u})\mathbf{I}\right] = -{}^{2P}/_{\omega}\,\mathbf{S} \qquad \text{(Eq. 14)}$$

where P is the isotropic pressure, from which the temperature, T, can be defined using the ideal gas equation of state, $P = \rho T$, D is the dimension of the underlying lattice, and ω is the single-time relaxation factor from the BGK collision operator.

The expression for the kinematic viscosity, ν,is:

$$\nu = \left(\frac{1}{\omega} - \frac{1}{2}\right)\mathrm{T} \qquad \text{(Eq. 15)}$$

LBM-based Turbulence Modelling Categories

Turbulence modelling based on the Lattice Boltzmann Method is studied under three categories. DNS-based, LES-based, and RANS-based. DNS-LBM, appeared to be successful at simulating fully-resolved turbulent flows at low Reynolds number; however, this method is computationally impractical for high Re, due to the multiplicity of temporal and spatial physical scales in industrial applications. LES-LBM, appeared to be very encouraging initially. This approach is still hot in researches due to several unanswered problems within the general LES framework, such as sub-grid model determination, adaptive resolution techniques for achieving grid scale in local inertial range, appropriate boundary conditioning and appropriate wall model determination. RANS-LBM offer the most economical approach for computing complex turbulent industrial flows. This is the approach that we will take in the present study. Basically, the only change to the fluid algorithm in RANS-LBM approaches is in the computation of the viscosity where, in the presence of a contribution from eddy-viscosity, υ_T, the total viscosity, ν, becomes a dynamic quantity. This eddy-viscosity is the door into the incorporation of different existing RANS models, such as the algebraic models, one-equation models, two-equation models, and etc. [5,13,14]. We will get into more details in the following sections.

The Prandtl's Mixing Length Model

The Prandtl's Mixing Length model is amongst the algebraic, simplest models for describing turbulent flows. This model was the first successful calculation of a practical turbulent flow, achieved in the 1920s by Prandtl [18], who introduced the concept of mixing length for the determination of the eddy viscosity. Von Kármán [19,20] gave further contributions to the mixing-length approach. Prandtl [21] tied the eddy viscosity to the turbulent kinetic energy through the development of a separate transport equation, opening the way to the one-equation models, where the turbulence length scale is defined empirically and the turbulent kinetic energy is obtained from a specific transport equation.

As stated previously, the fluid algorithm in RANS-LBM approaches only differs in the computation of viscosity, where the total viscosity, ν, becomes a dynamic quantity in the presence of an eddy-viscosity contribution, ν_T,

$$\nu = \left(\frac{1}{\omega} - \frac{1}{2}\right)\mathrm{T} = \nu_T + \nu_0 = \frac{1}{\omega_T}\mathrm{T} + \left(\frac{1}{\omega_0} - \frac{1}{2}\right)\mathrm{T} \qquad \text{(Eq. 16)}$$

where, ν_0 represents the molecular viscosity. The local quantity ω_T determines the eddy-viscosity and is implemented with the BGK operator, using the definition, $\frac{1}{\omega} \equiv \frac{1}{\omega_T} + \frac{1}{\omega_0}$.

Using the Prandtl's Mixing Length model, we would have,

$$\nu_T = (\kappa l_{mix})^2 |S| \qquad \text{(Eq. 17)}$$

$$|S| = \left(S_{ij}S_{ij}\right)^{1/2} \quad \text{(Eq. 18)}$$

$$\mathbf{S} = \frac{1}{2}\left[\frac{\partial u_\beta}{\partial x_\alpha} + \frac{\partial u_\alpha}{\partial x_\beta}\right] \quad \text{(Eq. 19)}$$

where $|S|$ is the magnitude of the strain rate tensor for incompressible flows, and κ is the von Karman constant, $\kappa = 0.41$. Based on the Chapman-Enskog analysis of the strain rate tensor, the Turbulent Relaxation Factor is derived as follows,

$$\omega_T = \frac{2 * \omega_0}{\sqrt{1 + 4Q\omega_0^2} - 1} \quad \text{(Eq. 20)}$$

where Q is calculated as follows,

$$Q = \frac{(\kappa l_{mix})^2}{2\rho T^2} \quad \text{(Eq. 21)}$$

Consequently, the total relaxation factor would be as follows,

$$\omega = \frac{2 * \omega_0}{\sqrt{1 + 4Q\omega_0^2} + 1} \quad \text{(Eq. 22)}$$

The for the mixing length we would have, $l_{mix} = \min(y, \gamma\delta) = 0.22\ (0.5D_h)$, based on [17], and ignoring the near wall consequences. Although the mixing length can be implemented in a two-layer approach [5], for simplicity, we went on with this strategy for the present study.

The implementation details will be elaborated in the following sections.

Problem Description

For the purpose of turbulence simulation using the Lattice-Boltzmann Method, the primary focus of this work is on incorporating the algebraic Prandtl's Mixing Length Model. The case that we are looking at for this research is the flow that occurs around a circular cylinder at various Reynolds numbers. This has led to the investigation of various flow regimes that occur around the cylinder. The drag calculation has been used for validation purposes for two Re numbers. In addition, a comparison has been made on the flow contours around the case's obstacle, coming from analytical sketches and the present simulation.

Flow Around a Circular Cylinder

The incompressible viscous flow around a circular cylinder can be considered as a prototype of bluff-body flows and has been subject of intensive research for over 100 years. Despite the simplicity of the boundary conditions, a large variety of interesting phenomena are observed. These phenomena are associated with the oncoming potential flow, the boundary layer, the separation, the shear layer, the near-wake, the far-wake, the vortex dynamics, and the complex interactions thereof. The cylinder wake is an ideal test case for many experimental methods and numerical simulations due to abundantly available data. In engineering problems, the effective mixing in cylinder wakes is employed in heat exchangers and the well-defined periodicity is used in vortex counters as flux meters. The wake may, however, give rise to less desirable problems, e.g., the potentially destructive aeroelastic coupling between chimneys and the vortex street.

The properties of the wake behind a circular cylinder change significantly at certain Reynolds numbers in the laminar ($Re < 160$), transitional ($160 < Re < 260$) and turbulent ($Re > 260$) Reynolds-number regime. In this regard, the simulations for the present study are done for 7 Re numbers, 5 main study cases and 2 cases for validation purposes, to cover different flow phases. Based on the Re number, here is the classification for flow over a circular cylinder from [9,10], Fig 1.

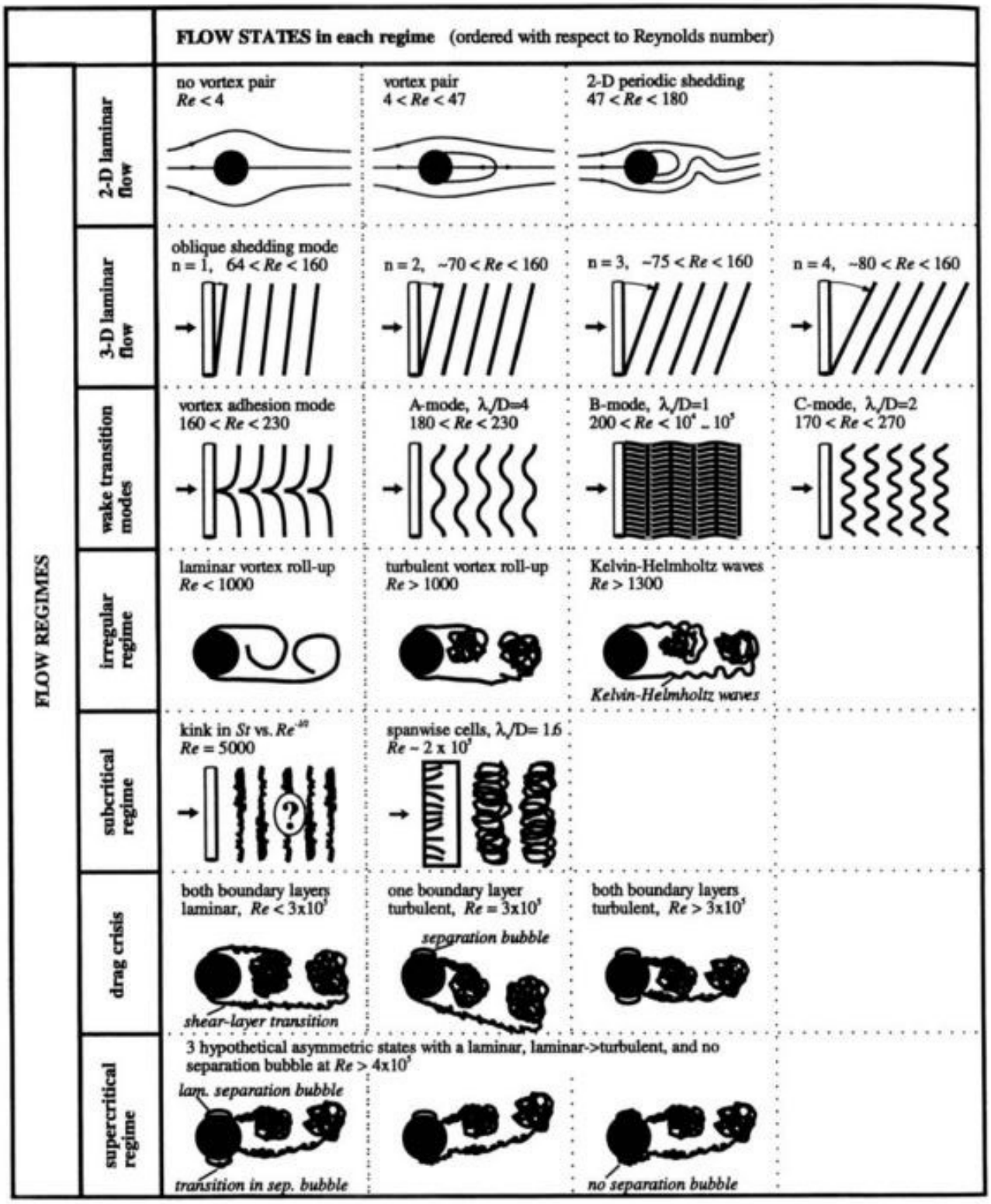

Figure 1- Laminar, transitional, and turbulent states of the flow around a circular cylinder, from [9,10]

Simulation Details

The microscopic particles that make up a fluid can be described with the distribution function $f(x, v)$, which describes the phase-space density of fluids at location x traveling with velocity v. The particles will do two things. Stream and collide. In this study, this behavior is captured by the BGKW approximation. The discretized Lattice-Boltzmann Equation with the BGKW approximation is as follows,

$$f_i(r + c_i\Delta t, t + \Delta t) = f_i(r, t) + \frac{\Delta t}{\tau}\left(f_i^{eq}(r, t) - f_i(r, t)\right) \quad \text{(Eq. 23)}$$

The local equilibrium distribution function with a relaxation time determines the type of problem needed to be solved. The beauty of this equation lies in its simplicity and can be applied for many physics by simply specifying a different equilibrium distribution function and source term (external force).

As stated previously, moments of the discrete distribution function can be taken to recover fluid variables at each lattice site.

Streaming

Streaming the particles is the first stage in the Lattice Boltzmann technique. This process is conceptually easy to follow. The value f_i is transferred to the adjacent lattice site along the connection for each lattice site for each direction i. Units of $\Delta t = \Delta x = 1$ are typically used in the Lattice Boltzmann technique, and we shall follow this convention throughout. The following are the flowing velocities: (0,0), (0,1), (0,-1), (1,0), (-1,0), (1,1), (1,1), (-1,1), (-1,-1).

Collisions

Next, the equilibrium state must be determined resulting from collisions. This relies on the equation of state of the fluid model. For the purpose of this study, an isothermal (constant temperature) fluid with a constant speed of sound is assumed. Using common conventions, the units are defined so that the lattice speed is c=1 (which equates to soundspeed2=1/3). The equilibrium condition is described by:

$$f_i^{eq} = \omega_i\rho\left(1 + 3(c_i \cdot u) + \frac{9}{2}(c_i \cdot u)^2 + \frac{3}{2}(u \cdot u)^2\right) \quad \text{(Eq. 24)}$$

which corresponds to the isothermal Navier-Stokes equations with a dynamic viscosity:

$$\mu = \rho\left(\tau - \frac{1}{2}\right)T \quad \text{(Eq. 25)}$$

where τ, represents the relaxation time, as, $\tau = {}^{1}/_{\omega}$.

Geometry and Study Cases

For this study, there are the following assumptions and considerations:

- Flow around 2D circular cylinder,
- Viscous, and Incompressible Flow (Mach Number < 0.3),
- Lattice-Boltzmann Method, BGKW Model,
- Chosen Lattice Arrangement D2Q9.

Figure 2, provide the parametric geometry, used for all of the simulations. The simulations differ from each other based on their resolution, domain and cylinder's size and the lattice velocity in order to represent a certain Re number. Table 1 provides the details of the simulations.

Table 1- Details of the simulation cases

Study Cases				
Re	nx	ny	Radius	Velocity
20	520	180	20	0.04
100	520	180	20	0.04
300	520	180	20	0.06
1010	520 × 2	450	50	0.06
1310	520 × 2	540	60	0.06
Validation Cases				
300	520	180	20	0.06
1000	520 × 2	540	60	0.06

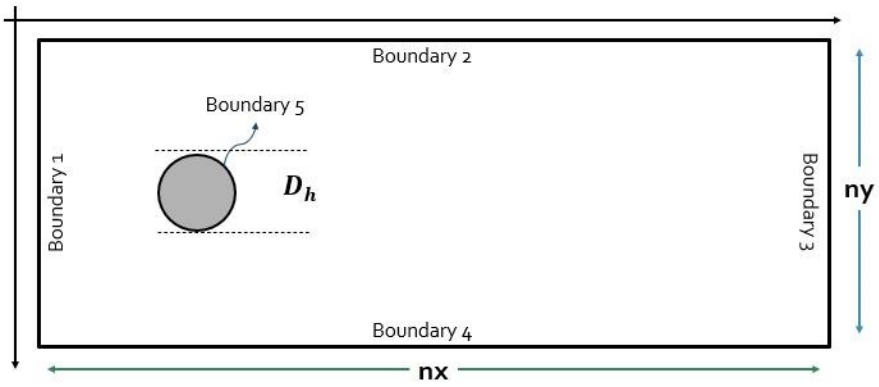

Figure 2- Geometry of the simulations with parametric dimensions

Boundary Conditions

For the boundary conditions, three different ways of treatment have been implemented. For the upper and lower boundaries, the Periodic Boundary Condition is implemented. This boundary condition asserts that the top and lower bounds are open and appropriate to the calculation of flow around a cylindrical object. For the Inflow and Outflow boundaries there exist a challenge. It is known that the left and right boundaries are velocity boundary conditions; hence, the distribution function of the lattice points on the left boundary are computed using the Zou-He boundary condition (There is a Re restriction for such a condition (Re<3900) which is preserved in the present study). Therefore, the left and right boundary values at the beginning of each cycle must be recalculated. The boundary condition on the cylindrical obstacle is the Bounce-back boundary condition to represent the no-slip condition. It is known that during the diffusion process, the particles of fluid node will enter the solid node in the direction of i and the particles of solid node will enter the fluid node in the direction of -i. The rebound format reverses the direction of particles entering the solid node.

Validation

In order to verify the code and validate the results of the present study, two test cases have been selected. The flow around a 2d, circular cylinder was simulated at Re numbers of 20, and 300 (in the Laminar, and turbulent regimes, respectively) and compared with results from experiments [7,11], and the numerical finite element method (FEM) from [8]. Table 2 provides the comparison between the outcomes. The results demonstrates that the findings of the present study provide acceptable accuracy in drag prediction for laminar regime, while deviates from accurate result for the turbulent regime which was predictable when using an algebraic model for turbulence modelling.

Table 2 - Drag coefficient comparison based on the present simulation results and results from the literature

Re	Cd (Experiment [7,8,11])	Cd (FEM [8])	% Of Error	Present Study – LBM	% Of Error
20	2.22	2.11	-4.9	2.38	+7.2
300	1.22	1.38	+13	0.8	-34

In order to better express the comparison between the results of this study with the literature [12], Table 3 provides the contours of flow over a 2d circular cylinder for the two selected Re numbers, 100, and 300. The results reveal that, while the algebraic model failed to predict the drag coefficient for the flow in turbulent regime with acceptable accuracy, it successfully has captured the general flow behavior behind the circular cylinder, both for the laminar and the turbulent regimes.

Table 3- Contours of flow over a 2d circular cylinder for the two selected Re numbers, 100, and 300, comparison between results from the present simulations and the literature, from [12]

Re	Present Simulation	From Literature (FVM)
100	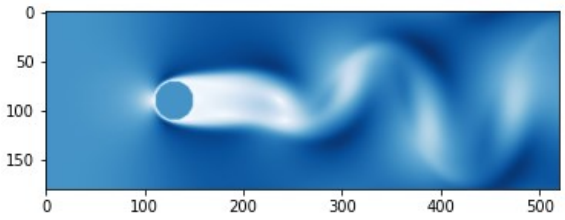	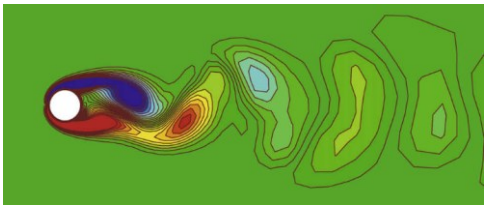
300	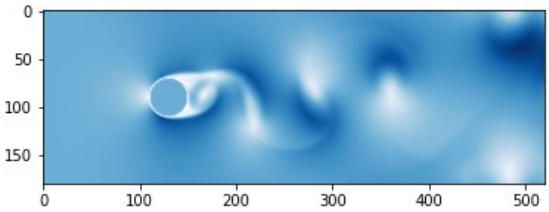	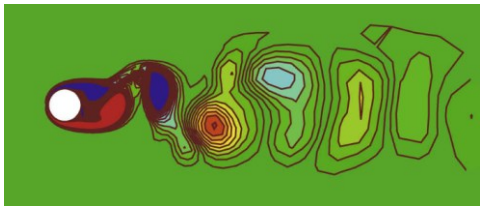

Results and Discussions

A cylinder's circular incompressible viscous flow can be viewed as a model for bluff-body flows. In this study, the wake structure behind a circular cylinder has been computed for two-dimensional flow of different Re numbers. Table 4 provides a full comparison on the results from the present study with what is expected from theoretical predictions. It can be inferred from Table 4 that the simulations of the present study have successfully predicted the general flow behavior around the circular cylinder. Since the two-layer model have been reduced to a one-layer model, the near-wall characteristics haven't been captured in the simulations. This is probability a reason for high deviation of drag prediction from the experimental results in the validation studies.

Re	Simulation	Description
20	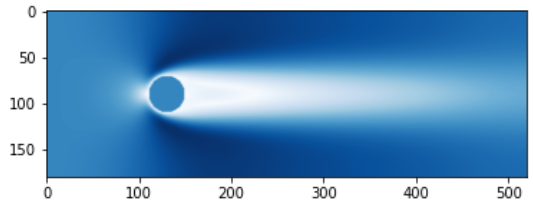	Vortex Pair
100	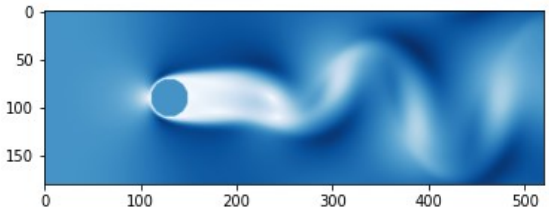	Periodic Shedding
300	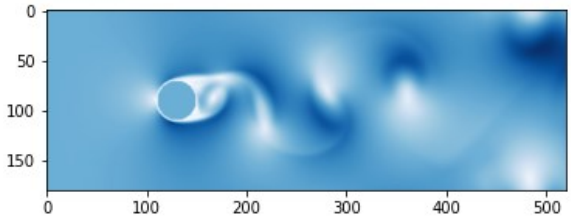	Laminar Vortex Roll-up
1010	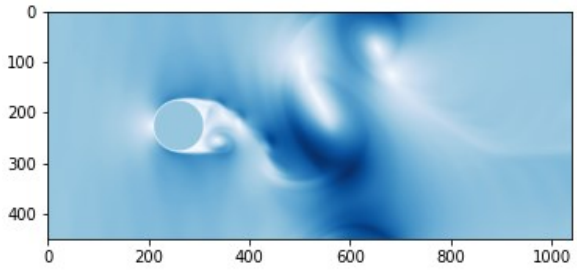	Turbulent Vortex Roll-up

1310	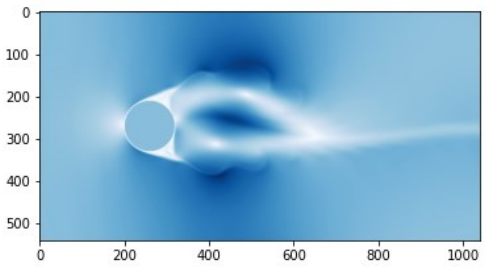	Kelvin-Helmholtz Waves

Conclusion

The primary reason for the development of new methods for simulating fluid dynamics that use a discrete, pseudo-microscopic approach, such as the Lattice-Gas Automata (LGA) or the Lattice-Boltzmann method (LBM) and its derivatives, is that the dynamics are simpler and more general than the approach that uses the continuum. This is a motivation that comes from the perspective of physics. By reducing the underlying physics in such a way that only the essential aspects (conservation laws, symmetry requirements, and correct equilibrium distributions) needed to guarantee accurate macroscopic behavior are maintained, it is possible to achieve a computational advantage over more traditional methods. In this regard, the Lattice Gaussian Approximation (LGA) and the Lattice Boltzmann (LB) approaches have been implemented in a variety of flow physics fields. Some examples include directly simulated or modeled single-phase turbulent flows, flows in complex geometries, multiphase and multicomponent flows, and flows that are undergoing heat transfer and chemical reactions.

For the purpose of turbulence simulation using the Lattice-Boltzmann Method, the primary focus of this work was on incorporating the algebraic Prandtl's Mixing Length Model. The flow that occurs around a circular cylinder at various Reynolds numbers have been studied extensively. This has led to the investigation of various flow regimes that occur around the cylinder. The circular incompressible viscous flow in a cylinder can be used as a metaphor for bluff-body flows. In this study, the wake structure after a cylinder in two dimensions with various Re numbers has been calculated. Based on the study's findings, it was concluded that simulations were successful in foretelling the overall flow behavior around the circular cylinder. The simulations have not taken into account the near-wall properties because the two-layer model has been reduced to a one-layer model. This is most likely the cause of the high difference between the drag prediction and the experimental findings in the validation experiments.

References

1. Mohamad, A. A. (2011). Lattice Boltzmann method (Vol. 70). London: Springer.
2. Website, https://palabos.unige.ch/get-started/lattice-boltzmann/
3. Website, https://medium.com/swlh/create-your-own-lattice-boltzmann-simulation-with-python-8759e8b53b1c
4. Website, https://programmer.ink/think/61f9324c5e5e3.html
5. Teixeira, C. M. (1998). Incorporating turbulence models into the lattice-Boltzmann method. International Journal of Modern Physics C, 9(08), 1159-1175.

6. Latt, J., Malaspinas, O., Kontaxakis, D., Parmigiani, A., Lagrava, D., Brogi, F., & Chopard, B. (2021). Palabos: parallel lattice Boltzmann solver. Computers & Mathematics with Applications, 81, 334-350.

7. Tritton, D.J.: Experiments on the flow past a circular cylinder at low Reynolds numbers. J. Fluid Mech. 6(4), 547–555 (1959).

8. Ostapenko, A., & Bulanchuk, G. (2018). Calculations of the drag coefficient of circular, square and rectangular cylinders using the lattice Boltzmann method with variable lattice speed of sound. Afrika Matematika, 29(1), 137-147.

9. Noack, B. R. (1999). On the flow around a circular cylinder. Part I: laminar and transitional regime. ZAMM-Journal of Applied Mathematics and Mechanics/Zeitschrift für Angewandte Mathematik und Mechanik, 79(S1), 223-226.

10. Noack, B. R. (1999). On the flow around a circular cylinder. Part II: turbulent regime. ZAMM-Journal of Applied Mathematics and Mechanics/Zeitschrift für Angewandte Mathematik und Mechanik, 79(S1), 227-230.

11. Rahman, M. M., Karim, M. M., & Alim, M. A. (2007). Numerical investigation of unsteady flow past a circular cylinder using 2-D finite volume method. Journal of Naval Architecture and Marine Engineering, 4(1), 27-42.

12. Rajani, B. N., Kandasamy, A., & Majumdar, S. (2009). Numerical simulation of laminar flow past a circular cylinder. Applied Mathematical Modelling, 33(3), 1228-1247.

13. Jahanshaloo, L., Pouryazdanpanah, E., & Che Sidik, N. A. (2013). A review on the application of the lattice Boltzmann method for turbulent flow simulation. Numerical Heat Transfer, Part A: Applications, 64(11), 938-953.

14. Pellerin, N., Leclaire, S., & Reggio, M. (2015). An implementation of the Spalart–Allmaras turbulence model in a multi-domain lattice Boltzmann method for solving turbulent airfoil flows. Computers & Mathematics with Applications, 70(12), 3001-3018.

15. Alfonsi, G. (2009). Reynolds-averaged Navier–Stokes equations for turbulence modeling. Applied Mechanics Reviews, 62(4).

16. Chapman, S., & Cowling, T. G. (1990). The mathematical theory of non-uniform gases: an account of the kinetic theory of viscosity, thermal conduction and diffusion in gases. Cambridge university press.

17. Patankar, S. V., & Spalding, D. B. (1968). Heat and mass transfer in boundary layers. Morgan-Grampian.

18. Prandtl, L., 1925, "Über die ausgebildete Turbulenz," Z. Angew. Math. Mech., 5, pp. 136–139.

19. von Kármán, T., 1930, "Mechanische Ähnlichkeit und Turbulenz," 3rd Inter- national Congress of Applied Mechanics, Stockholm, pp. 85–105.

20. von Kármán, T., 1948, "Progress in the Statistical Theory of Turbulence," Proc. Natl. Acad. Sci. U.S.A., 34, pp. 530–539.

21. Prandtl, L., 1945, "Über ein neues Formelsystem für die augebildete Turbu- lenz," Nachr. Akad. Wiss. Goett. II, Math.-Phys., K1, pp. 6–19.